Inorganic Chemistry

pubs.acs.org/IC

Communication

Unexpected Imidazole Coordination to the Dirhodium Center in a Protein Environment: Insights from X-ray Crystallography and Quantum Chemistry

Domenico Loreto,[†] Francesca Fasulo,[†] Ana B. Muñoz-García, Michele Pavone,* and Antonello Merlino*

Cite This: *Inorg. Chem.* 2022, 61, 8402−8405

Read Online

ACCESS | Metrics & More | Article Recommendations | Supporting Information

ABSTRACT: X-ray diffraction data demonstrate that the adduct formed upon the reaction of dirhodium(II,II) tetraacetate with RNase A reacts with imidazole, leading to the formation of an unexpected product with the imidazole that binds the dirhodium center at an equatorial site rather than an axial site. The origin of this result has been dissected using quantum-chemical calculations.

Dirhodium(II) complexes with bridging equatorial ligands, such as $[Rh_2(\mu\text{-}O_2CR)_4]L_2$ (R = Me, Et, Pr; L = axially coordinated solvent), are cytotoxic compounds and efficient catalysts for a number of reactions,[1−7] including hydrogen evolution and CO_2 reduction.[8−10] It is generally accepted that the reaction of $[Rh_2(\mu\text{-}O_2CCH_3)_4]$ with nitrogen-containing ligands (L_N) produces axially substituted $[Rh_2(\mu\text{-}O_2CCH_3)_4](L_N)_2$ species.[11−13] In particular, when L_N is imidazole (Im), the $[Rh_2(\mu\text{-}O_2CCH_3)_4](Im)_2$ species forms; the X-ray structure of this species has been reported.[13]

We have recently proven by several experimental techniques, including X-ray crystallography, that $[Rh_2(\mu\text{-}O_2CCH_3)_4]$ reacts with the model protein bovine pancreatic ribonuclease (RNase A), forming adducts with the side chains of His105 and His119 that coordinate the dirhodium center at the axial site.[14,15] In these adducts, over time, the acetate ligands are mostly replaced by water molecules.[14,15] With the aim of verifying the dirhodium compound reactivity upon formation of the adduct with the protein at the crystal state, here we solved the X-ray structure of the reaction product of the dirhodium tetraacetate/RNase A system with Im. This represents a rare example of *in crystallo* reactivity of a metal/protein adduct.

Crystals of the adduct formed upon the reaction of dirhodium tetraacetate with RNase A were prepared according to the previously reported procedure.[14] These crystals were then treated with a solution of Im dissolved in the reservoir. X-ray diffraction data on these crystals were collected at the XRD2 beamline of Elettra synchrotron, Trieste, Italy. Data collection and refinement statistics are reported in Table S1. The structure, which was solved at 1.40 Å resolution and refined to a *R* factor of 18.9 (*R*-free 23.1), contains two molecules in the asymmetric unit (molecules A and B; Figure S1). The final model was deposited in the Protein Data Bank under the accession code 7QHR. The two molecules in the asymmetric unit are very similar to each other (root-mean-square deviation, rmsd, between equivalent carbon α atoms is as low as 0.39 Å) and to those in the crystal of the adduct of the protein with dirhodium tetraacetate (rmsd = 0.22 and 0.15 Å for molecules A and B, respectively).

As expected, the dirhodium center is found close to the side chains of His105 and His119 in both molecules A and B (Figures S2−S4 and 1). Close to the dirhodium core bound to the side chain of His119 of molecules A and B, three acetate ions and two water molecules are found at the equatorial dirhodium sites, while a water molecule is found at the axial site (Figures S2 and S3). Analysis of the electron density maps reveals that, close to the dirhodium centers coordinated to the side chains of His105 of the two protein molecules in the asymmetric unit, an Im ligand is found. Interpretation of the electron density map in molecule A is complicated by the presence of alternative conformations of the dirhodium-containing fragment (Figure S4). However, in molecule B, this site is very well-defined. Surprisingly, Im does not bind the dirhodium center at the axial coordination site, as expected, but it coordinates one of the two rhodium atoms of the dimetallic core at the equatorial site (Figure 1). The Im binding to the dirhodium center is stabilized by a network of hydrogen bonds and contacts that the heterocycle compound forms with surrounding residues and solvent molecules (Figure 1). The (di)rhodium coordination sphere is completed by water molecules and an acetate ligand (Figure 1).

To shed light on the origin of this unexpected experimental evidence, we investigated the reactivity and selectivity of the observed dirhodium tetraacetate/protein adduct (at His105) with a second Im by quantum chemistry,[17−19] within the framework of density functional theory (DFT; see the computational details in the Supporting Information).

Following the cluster approach recently reviewed by Himo and co-workers,[20,21] we carved from the crystal structure a

Received: April 26, 2022
Published: May 24, 2022

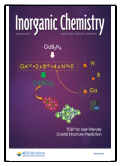

https://doi.org/10.1021/acs.inorgchem.2c01370
Inorg. Chem. 2022, 61, 8402−8405

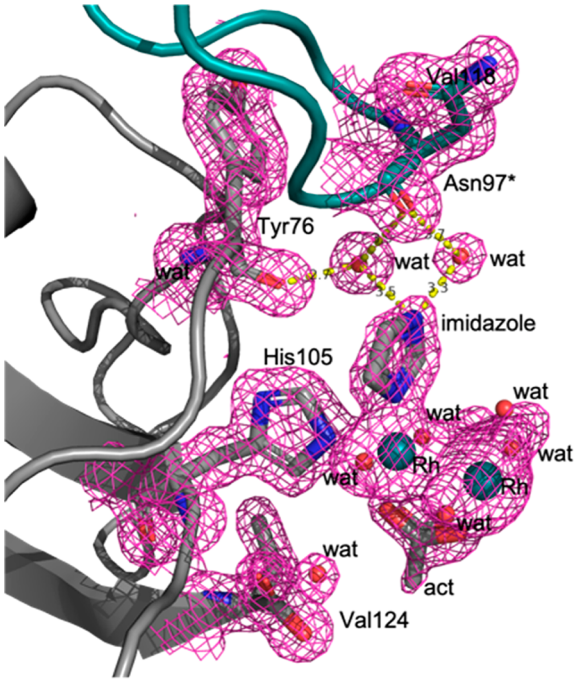

Figure 1. Im binding site in the structure of RNase A treated with $[Rh_2(\mu\text{-}O_2CCH_3)_4]$ and then with Im. The dirhodium center is coordinated to the side chain of His105. The $2F_o - F_c$ electron density map is reported at 1.0 σ and colored in pink.

small portion of the dirhodium/protein adduct around the His105 residue (for cluster model, see Figure 2a). We built this model based on simple considerations on the distance of the surrounding residues from the dirhodium core. We also applied, for a comparison, a simplified minimal model where the protein environment is neglected, and we only considered an Im molecule at the axial position, mimicking the coordination of His105. In both cases, we also used implicit solvation via the polarizable continuum model to account for the dielectric properties of the chemical environment. We selected water as the solvent because the dirhodium adduct is exposed to aqueous solution and it is almost fully hydrolyzed. For both models, we characterized coordination of the second Im molecule to the three available sites: the axial site opposite to His105/Im (ax), equatorial to the second rhodium atom (r2) and equatorial to the rhodium atom that is already coordinated by His105/Im (r), as depicted by Figure 2.

The free energies for all of these substitutions were computed according to eq 1 and are listed in Table 1.

$$Rh_2(His/Im)(\mu\text{-}O_2CCH_3)(H_2O)_7 + Im \rightarrow Rh_2(His/Im)(Im)_{ax/r2/r}(\mu\text{-}O_2CCH_3)(H_2O)_6 + H_2O \quad (1)$$

As clearly highlighted by the computational data, there is a specific preference for Im coordination to the equatorial site (r), in agreement with experiments. Comparing the cluster and minimal models, we can find that the presence of the surrounding protein residues improves the thermodynamic driving force for coordination at the (r) site with respect to the other two options. However, we must note that the minimal model is indeed able to catch the correct binding trend, and so it can be used further to rationalize this process.

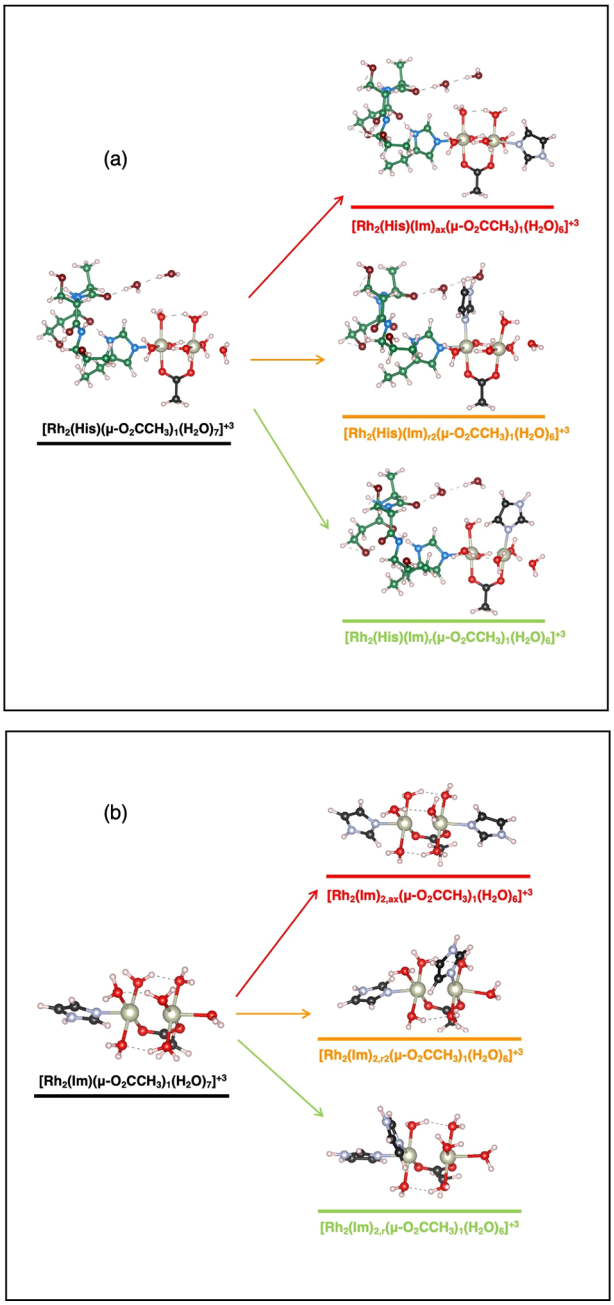

Figure 2. Substitution reactions with inclusion of the second Im molecule for the dirhodium/protein adduct (cluster model) (a) and for the corresponding minimal model (b). Legend: Rh, silver; O, red; N, light blue; C, green/black; H, white.

Table 1. Free-Energy Variations (ΔG) upon Substitution of a Water Molecule (eq 1) with Im at Different Coordination Sites and Relative Free Energy Variations (ΔG_{rel}) with Respect to the Experimentally Found Equatorial Site (r)

		ax	r2	r
ΔG (eV)	cluster model	−0.398	−1.004	−1.173
	minimal model	−0.482	−0.940	−1.003
ΔG_{rel} (eV)	cluster model	0.776	0.169	0.0
	minimal model	0.544	0.081	0.0

First, we considered the formation of hydrated species, where six water molecules replaced three tetraacetate groups,

https://doi.org/10.1021/acs.inorgchem.2c01370
Inorg. Chem. 2022, 61, 8402−8405

as found in the protein environment. We found that the cost of removing the three ligands is not balanced by coordination of the water molecules, and the free energy variation upon going from $[Rh_2(Im)(\mu\text{-}O_2CCH_3)_4(H_2O)]$ to $[Rh_2(Im)(\mu\text{-}O_2CCH_3)(H_2O)_7]$ is positive (i.e., unfavorable) with a value of ∼5 eV (Figure S5). Our calculations considered that the acetate groups enter into the solvent as isolated moieties. The protein environment, evidently, balanced the thermodynamics for this process by providing convenient coordination spots for the leaving acetate groups, and concurrently it also provided extra stabilization via the second-shell hydrogen-bond network. From the hydrated species $[Rh_2(Im)(\mu\text{-}O_2CCH_3)(H_2O)_7]$, where the axial Im molecule is modeling the His105 side chain, the second Im molecule favorably substitutes the water molecule at the (r) equatorial site, in agreement with the experiments.

The reason behind such unexpected Im binding can be found in the electronic features of the $[Rh_2(Im)(\mu\text{-}O_2CCH_3)(H_2O)_7]$ compound, where the two rhodium atoms are not equivalent because of the presence of the Im(His105) ligand, as depicted by Figure 3. Bader's Atom-in-Molecule charge

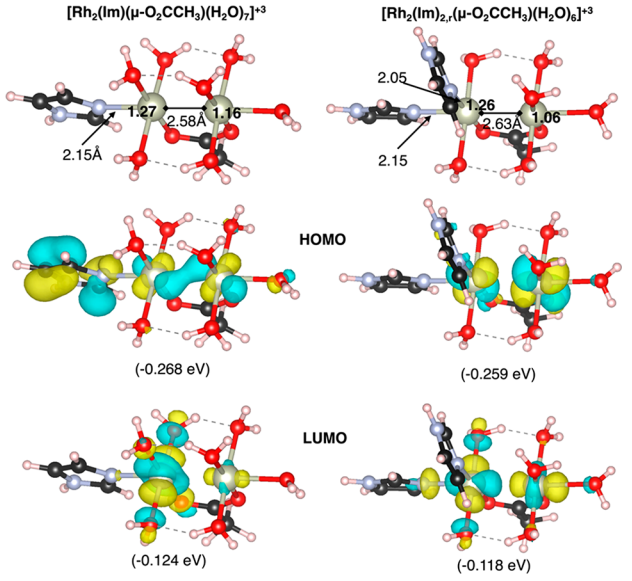

Figure 3. Top panel: Computed Bader charges on rhodium atoms and selected distances for $[Rh_2(Im)(\mu\text{-}O_2CCH_3)(H_2O)_7]$ and $[Rh_2(Im)_{2,r}(\mu\text{-}O_2CCH_3)(H_2O)_6]$. Central (bottom) panel: HOMO (LUMO) of both adducts and corresponding energies. Color code as in Figure 2, in which the isodensity surfaces are depicted as yellow and cyan for positive and negative values, respectively. The distances and Bader's effective charges are reported for rhodium in the top panel, and the HOMO and LUMO energies are reported in parentheses.

analysis of the starting compounds (Figure 3, top panel) shows that the rhodium bound to Im(His) is slightly more positive than the other rhodium, and thus it can act as a better Lewis acid site for the second Im.

It is worth noting that the degree of hydrolysis also plays a noninnocent role in the observed and computed selectivity. We calculated the substitution free energies for a water molecule by Im on different sites also for the $[Rh_2(Im)(\mu\text{-}O_2CCH_3)_4(H_2O)]$, $[Rh_2(Im)(\mu\text{-}O_2CCH_3)_3(H_2O)_3]$, and $[Rh_2(Im)(\mu\text{-}O_2CCH_3)_2(H_2O)_5]$ series, i.e., for adducts with four, three, and two acetate ligands, to be compared to the highly hydrolyzed $[Rh_2(Im)(\mu\text{-}O_2CCH_3)(H_2O)_7]$ considered above. We found that configurations with the second Im at the axial position are by far the least favorable for all hydrolysis degrees (Figure S5). However, regarding the equatorial positions, $(Im)_{2,r2}$-like configurations are slightly preferred over $(Im)_{2,r}$ ones for adducts with three and two acetate groups. The experimentally obtained $(Im)_{2,r}$ one becomes the most stable only for the adduct with one acetate group. Of course, the presence of a second-shell hydrogen-bonding network with protein residues can alter these relative energies. However, it is already proven that the protein itself has the key role of sufficiently hydrolyzing the tetraacetate compound,[14−16] so that when Im is added, the final $(Im)_{2,r}$ is formed.

The new dirhodium complex has peculiar electronic features that can result in modified (photo)catalytic activity, as shown by the qualitative differences in computed frontier orbitals of $[Rh_2(Im)_{2,r}(\mu\text{-}O_2CCH_3)(H_2O)_6]$ with respect to $[Rh_2(Im)(\mu\text{-}O_2CCH_3)(H_2O)_7]$ (Figure 3). For example, the involvement in the highest occupied molecular orbital (HOMO) of the Im ligand π system in $[Rh_2(Im)(\mu\text{-}O_2CCH_3)(H_2O)_7]$ is lost in $[Rh_2(Im)_{2,r}(\mu\text{-}O_2CCH_3)(H_2O)_6]$, and the lowest unoccupied molecular orbital (LUMO) presents a more significant contribution from the second rhodium than in the single Im complex (Figure 3). Further experimental and theoretical characterizations of the photophysical and/or catalytic properties of this new dirhodium center are ongoing in our laboratory.

In conclusion, we characterized from the structural point of view the product of the reaction of a dirhodium/protein adduct with Im. Interestingly, at solid state the dirhodium complex reacts with Im, forming an unexpected product, with Im bound at the equatorial position. This result can have important implications considering that $[Rh_2(\mu\text{-}O_2CCH_3)_4]$ binds human serum albumin, the most abundant plasma protein, through coordination to histidine residues,[13] and that the binding deeply affects the metal compound efficacy as an anticancer agent. The reaction mechanism was elucidated by quantum-chemical calculations. DFT results predict the same coordination complex as in experiments to be the most stable once the original dirhodium complex undergoes hydrolyzation during formation of the adduct with the protein. The origin of the observed unexpected preference toward coordination of the Im moiety to the equatorial position is unveiled by electronic structure analysis, which also highlights peculiar features of frontier molecular orbitals. Our combined experimental and theoretical results pave the way to further investigations of this unprecedented protein-bound dirhodium center, opening at the same time new directions in the exploitation of the crystal reactivity toward new coordination complexes of transition-metal cations.

■ ASSOCIATED CONTENT

Supporting Information

The Supporting Information is available free of charge at https://pubs.acs.org/doi/10.1021/acs.inorgchem.2c01370.

Experimental section, crystallography, DFT, Figures S1−S5, and Tables S1 and S2 (PDF)

https://doi.org/10.1021/acs.inorgchem.2c01370
Inorg. Chem. 2022, 61, 8402−8405

AUTHOR INFORMATION

Corresponding Authors

Michele Pavone − *Department of Chemical Sciences, University of Naples Federico II, Napoli I-80126, Italy;* orcid.org/0000-0001-7549-631X; Email: michele.pavone@unina.it

Antonello Merlino − *Department of Chemical Sciences, University of Naples Federico II, Napoli I-80126, Italy;* orcid.org/0000-0002-1045-7720; Email: antonello.merlino@unina.it

Authors

Domenico Loreto − *Department of Chemical Sciences, University of Naples Federico II, Napoli I-80126, Italy*

Francesca Fasulo − *Department of Chemical Sciences, University of Naples Federico II, Napoli I-80126, Italy*

Ana B. Muñoz-García − *Department of Physics "Ettore Pancini", University of Naples Federico II, Napoli I-80126, Italy;* orcid.org/0000-0002-9940-7358

Complete contact information is available at: https://pubs.acs.org/10.1021/acs.inorgchem.2c01370

Author Contributions

†These authors contributed equally.

Notes

The authors declare no competing financial interest.

ACKNOWLEDGMENTS

The authors thank Elettra synchrotron staff for technical assistance during data collection.

REFERENCES

(1) Hrdina, R. Dirhodium(II,II) Paddlewheel Complexes. *Eur. J. In. Chem.* **2021**, *6*, 501−528.

(2) Davies, H. M. L.; Manning, J. R. Catalytic C—H Functionalization by Metal Carbenoid and Nitrenoid Insertion. *Nature* **2008**, *451*, 417−424.

(3) Che, C.-M.; Lo, V. K.-Y.; Zhou, C.-Y.; Huang, J.-S. Selective Functionalisation of saturated C—H bonds with metalloporphyrin catalysts. *Chem. Soc. Rev.* **2011**, *40*, 1950−1975.

(4) Breslow, R.; Gellman, S. H. Intramolecular Nitrene Carbon-hydrogen Insertions Mediated by Transition-metal Complexes as Nitrogen Analogs of Cytochrome P-450 reactions. *J. Am. Chem. Soc.* **1983**, *105*, 6728−6729.

(5) Liu, W.; Kuang, Y.; Wang, Z.; Zhu, J.; Wang, Y. Dirhodium(II)-catalyzed [3 + 2] Cycloaddition of N-arylaminocyclopropane with Alkyne Derivatives. *Beilstein J. Org. Chem.* **2019**, *15*, 542−550.

(6) Kataoka, Y.; Yano, N.; Kohara, Y.; Tsuji, T.; Inoue, S.; Kawamoto, T. Experimental and Theoretical Study of Photochemical Hydrogen Evolution Catalyzed by Paddlewheel-Type Dirhodium Complexes with Electron Withdrawing Carboxylate Ligands. *Chem. Catal. Chem.* **2019**, *11*, 6218−6226.

(7) Tanaka, S.; Masaoka, S.; Yamauchi, K.; Annaka, M.; Sakai, K. Photochemical and Thermal Hydrogen Production from Water Catalyzed by Carboxylate-bridged Dirhodium(ii) Complexes. *Dalton Trans.* **2010**, *39*, 11218−11226.

(8) Millet, A.; Xue, C.; Turro, C.; Dunbar, K. R. Unsymmetrical Dirhodium Single Molecule Photocatalysts for H Production with Low Energy Light. *Chem. Commun.* **2021**, *57*, 2061−2064.

(9) Huang, J.; Sun, J.; Wu, Y.; Turro, C. Dirhodium(II,II)/NiO Photocathode for Photoelectrocatalytic Hydrogen Evolution with Red Light. *J. Am. Chem. Soc.* **2021**, *143*, 1610−1617.

(10) Huang, J.; Gallucci, J. C.; Turro, C. Panchromatic Dirhodium Photocatalysts for Dihydrogen Generation with Red Light. *Chem. Sci.* **2020**, *11*, 9775−9783.

(11) Bocian, W.; Jaźwiński, J.; Sadlej, A. 1H, 13C and 15N NMR Studies on Adducts Formation of Rhodium(II) Tetraacylates with some Azoles in $CDCl_3$ Solution. *Magn. Reson. Chem.* **2008**, *46* (2), 156−165.

(12) Jaźwiński, J.; Kamienski, B. Adducts of Rhodium(II) Tetraacetate with some Nitrogenous Organic Ligands: Application of Natural Abundance 15N and 13C CPMAS NMR Spectroscopy. *Solid State Nucl. Magn. Reson.* **2007**, *32*, 25−33.

(13) Jalilehvand, F.; Enriquez Garcia, A.; Niksirat, P.; Finfrock, Y. Z.; Gelfand, B. S. Binding of Histidine and Human Serum Albumin to Dirhodium(II)tetraacetate. *J. Inorg. Biochem.* **2021**, *224*, 111556.

(14) Ferraro, G.; Pratesi, A.; Messori, L.; Merlino, A. Protein Interactions of Dirhodium Tetraacetate: A Structural Study. *Dalton Trans.* **2020**, *49*, 2412−2416.

(15) Loreto, D.; Merlino, A. The Interaction of Rhodium Compounds with Proteins: A Structural Overview. *Coord. Chem. Rev.* **2021**, *442*, 213999.

(16) Loreto, D.; Ferraro, G.; Merlino, A. Unusual Structural Features in the Adduct of Dirhodium Tetraacetate with Lysozyme. *Int. J. Mol. Sci.* **2021**, *22*, 1496.

(17) Kataoka, Y.; Kitagawa, Y.; Saito, T.; Nakanishi, Y.; Sato, K.; Miyazaki, Y.; Kawakami, T.; Okumura, M.; Mori, W.; Yamaguchi, K. Theoretical Study of Absorption Spectrum of Dirhodium Tetracarboxylate Complex $[Rh_2(CH_3COO)_4(H_2O)_2]$ in Aqueous Solution Revisited. *Supr. Chem.* **2011**, *23*, 329−336.

(18) Burda, J. V.; Gu, J. A Computational Study on DNA Bases Interactions with Dinuclear Tetraacetato-diaqua-dirhodium(II,II) complex. *J. Inorg. Biochem.* **2008**, *102*, 53−62.

(19) Adamo, C.; Lelj, F. A Hybrid Density Functional Study of the First-row Transition-metal Monocarbonyls. *J. Chem. Phys.* **1995**, *103*, 10605−10613.

(20) Himo, F. Recent Trends in Quantum Chemical Modeling of Enzymatic Reactions. *J. Am. Chem. Soc.* **2017**, *139*, 6780−6786.

(21) Siegbahn, P. E. M.; Himo, F. The quantum chemical cluster approach for modeling enzyme reactions. *WIREs Comput. Mol. Sci.* **2011**, *1*, 323−336.

NOTE ADDED AFTER ASAP PUBLICATION

This paper was published ASAP on May 24, 2022. Figure 2 was replaced due to minor errors in panel b, and the corrected version was reposted on May 25, 2022.

https://doi.org/10.1021/acs.inorgchem.2c01370
Inorg. Chem. 2022, 61, 8402−8405